



HHS Public Access

Author manuscript

Colloids Surf A Physicochem Eng Asp. Author manuscript; available in PMC 2022 October 01.

Published in final edited form as:

Colloids Surf A Physicochem Eng Asp. 2022 October ; 650: . doi:10.1016/j.colsurfa.2022.129611.

Iron-containing metal-organic framework thin film as a drug delivery system

Angela Bui,

Steven G. Guillen,

Andy Sua,

Travis C. Nguyen,

Angel Ruiz,

Lester Carachure,

Mark D.R. Weber,

Araseli Cortez,

Fangyuan Tian*

Department of Chemistry and Biochemistry, California State University Long Beach, Long Beach, CA 90840, USA

Abstract

Selective bulk metal-organic frameworks (MOFs) have exhibited great potential in biomedical applications. However, topical treatments and drug elution coatings will require uniform films as drug delivery systems. This work studies the use of surface supportive MOF thin films for drug loading and releasing. More specifically, we focus on an iron-containing MOF, MIL-88B(Fe), on a COOH-terminated self-assembled monolayer (SAM) modified Au surface for encapsulating ibuprofen as a model drug. A combined experimental and computational approach was employed to study the fabrication of MIL-88B(Fe) film on functionalized Au surfaces. We used several surface characterization techniques, including infrared spectroscopy and scanning electron microscopy, to confirm the chemical composition and morphological changes of the surface after each modification step. The resulting MIL-88B(Fe) thin film was found capable of loading 8.7 wt% of ibuprofen using quartz crystal microbalance analysis. Moreover, we applied cluster simulations to study the binding mechanisms of MIL-88B(Fe) and its interactions with ibuprofen based on the density functional theory (DFT). The unsaturated Fe site was confirmed

This is an open access article under the CC BY-NC-ND license (<http://creativecommons.org/licenses/by-nc-nd/4.0/>).

*Corresponding author: fangyuan.tian@csulb.edu (F. Tian).

CRediT authorship contribution statement

Angela Bui: Methodology, Investigation, Writing – original draft. **Steven G. Guillen:** Software, Formal analysis, Writing – original draft. **Andy Sua:** Investigation, Writing – original draft. **Travis C. Nguyen:** Validation. **Angel Ruiz:** Validation. **Lester Carachure:** Methodology. **Mark D. R. Weber:** Investigation. **Araseli Cortez:** Validation. **Fangyuan Tian:** Conceptualization, Supervision, Writing – original draft, Writing – review & editing, Funding acquisition.

Declaration of Competing Interest

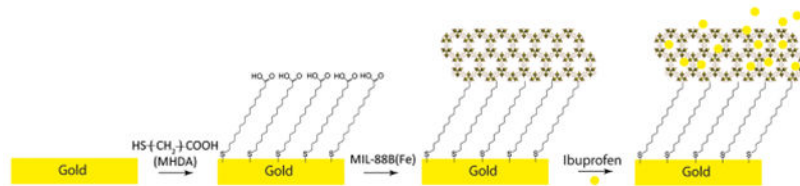
The authors declare that they have no known competing financial interests or personal relationships that could have appeared to influence the work reported in this paper.

Appendix A. Supporting information

Supplementary data associated with this article can be found in the online version at doi:[10.1016/j.colsurfa.2022.129611](https://doi.org/10.1016/j.colsurfa.2022.129611).

kinetically more favorable to bind to the COOH-end group on the SAM. Hydrogen bonding and π -CH interactions between ibuprofen and MIL-88B(Fe) promote ibuprofen being retained inside of the cages of MIL-88B(Fe).

GRAPHICAL ABSTRACT



Keywords

Metal-organic frameworks (MOFs); Drug delivery; Quartz crystal microbalance (QCM); Density functional theory (DFT); surface modification

1. Introduction

An increasing need for development in non-toxic thin films has been driven by the manufacturing of oral strips and medical implants for drug delivery. This work studies a surface-supportive iron-based metal-organic framework (MOF) thin films for releasing therapeutic agents. As relatively new porous materials, MOFs have attracted considerable amount of attention in the last two decades due to their exceptional high internal surface areas, versatile structures, and excellent catalytic properties [1–3]. Generally, MOFs are highly coordinated porous structures consisting of isolated metal ions or clusters linked with organic ligands forming one to three-dimensional cages [4]. Furthermore, MOFs have been investigated for a variety of practices including gas sensing, separation and storage, catalysis, water remediation, and other health-related applications [5–13].

One type of MOF, MIL-88 (MIL stands for Material from Institute Lavoisier) along with other Fe-based MOFs, have been recently studied and identified as suitable carriers for the loading of various therapeutic molecules, including doxorubicin, ibuprofen, caffeine, etc.[14–16]. In general, MIL-88 is composed of trivalent transition metal clusters (M₃, μ_3 -O) connected with aliphatic or aromatic dicarboxylate groups, including fumarate (MIL-88A), terephthalate (MIL-88B), 2,6-naphthale-nedicarboxylate (MIL-88 C), and biphenyldicarboxylate (MIL-88D) [17]. Serre et al. first reported the synthesis of MIL-88 and MIL-89 by a controlled secondary building unit approach [17,18]. The general formula for MIL-88 and MIL-89 has been determined as M₃O(L)₃(H₂O)₂(X), where M represents Fe or Cr; L is the linear dicarboxylate ligands, and X is the anion (CH₃COO[−] for MIL-88 and CL for MIL-89, respectively).[18,19] Furthermore, Horcajada et al. discovered the “breathing effect” of MIL-88(Fe), which was described as the shrinking and enlargement of its cage volume as determined by the size of the guest molecule, all without affecting the structural integrity of the framework [19]. Understanding the structures of MIL-88 opens vast unexplored opportunities in the fields of gas capture, delivery of nitric oxide, drug encapsulation, and more [20–22]. Studies of the first Fe-based MOFs provided evidence

Author Manuscript

Author Manuscript

Author Manuscript

Author Manuscript

that MIL-100 and MIL-101(Fe) were suitable for drug delivery applications; where each material was noted to contain a large and flexible cavity capable of remarkably high drug storage (1.376 g of ibuprofen per gram of MIL-101 and 0.347 g of ibuprofen per gram of MIL-100) [23]. Two years later, the same group reported a study of using another flexible MOF, MIL-53(Fe), for drug encapsulation utilizing ibuprofen as a model drug. MIL-53(Fe) exhibited a high loading efficacy of 0.210 g of ibuprofen per gram of MOF and a steady drug releasing profile over 3 weeks [24]. The structural flexibility of these Fe-based MILs enable them to adjust their cage volume when loading drug molecules with various sizes, making the drug encapsulation process more efficient [22,25]. The Férey group have also reported several other Fe-based MIL materials (MIL-88A, MIL-88B, MIL-89, and MIL-101_NH₂) for delivery of various model drugs, including busulfan, azidothymidine triphosphate, cidofovir and doxorubicin [14]. Furthermore, Fe-based MILs exhibit low toxicity as confirmed by in vitro and in vivo toxicological studies, [26, 27] which is essential for drug delivery. Most Fe-based MILs have a hydrophobic core and a hydrophilic exterior, making them suitable for loading drugs that have low solubilities in aqueous solutions. Combining all the factors sets Fe-based MILs as promising candidates for drug delivery applications.

However, the above-mentioned bulk MOFs in powder form has limited their applications when a smooth layered drug delivery system is needed. For instance, a delicate yet robust thin film for drug releasing is critically important in medical implants, including drug-eluting stents (DES) metal alloys used in arthroplasty and hip replacement surgeries [28,29]. Therefore, it is important to fabricate bulk MOFs on surfaces to the form of thin films, known as surface-supported MOFs (SURMOFs) [30–32]. These SURMOFs can be prepared by both direct and indirect methods. With direct crystallization methods, the growth of MOF crystals originates from the synthesis solution or an aged mixture of reactants, producing a dense layer of SURMOFs. [33,34] Indirect liquid phase epitaxy methods, on the other hand, can produce a more homogeneous SURMOF thin film [35,36]. Liquid phase epitaxy approach, such as dip-coating and layer-by-layer (LbL) deposition, involves the immersion of a solid substrate into different reaction compound solutions in cycles.[37,38] However, MOFs with “paddlewheel” structures (a tetragonal symmetry) are more successfully prepared following the LbL method [39,40]. Moreover, recent work has suggested that the vacant apical positions of the paddlewheel metal nodes (usually dimeric metal, such as Cu, Zn, and Co) are critical binding sites prerequisite for thin film formation [41].

Unlike paddlewheel MOFs, Fe-MILs are composed of trimeric FeO₆ octahedral clusters coordinated with organic linkers. Thus, the challenge arises for binding Fe-MIL films directly onto metal substrates. To overcome this, a self-assembled monolayer (SAM) can be formed on a metal substrate prior to growing the Fe-MIL thin film. Scherb et al. reported a MIL-88B(Fe) film built on a 16-mercaptohexadecanoic acid (MHDA)-functionalized Au surface following a direct mother solution soaking method [42]. This COOH-terminated SAM is able to form coordination bonds with the central iron trimers, resulting in the growth of MIL-88B crystals along the [001] direction [42]. The same research group also found the cell volume of MIL-88B(Fe) thin film increased by over 40 % due to the elastic stress of the flexible host framework during water sorption [43]. This finding confirmed that both

bulk and thin film forms of Fe-based MIL-88 have excellent structural flexibility. More importantly, the low toxicity of Fe-based MIL-88B assures its applications in biomedical fields [27,44]. Our previous studies confirmed that MIL-88B(Fe) exhibits no adverse effects on cell viability up to 0.1 mg/mL tested with NIH-3T3 Swiss mouse fibroblasts [16]. As such, these discoveries open ample opportunities for using MOF thin films (MIL-88 specifically) for selective drug encapsulation.

In this study, we focused on building a MIL-88B(Fe) thin film on a SAM-modified Au substrate function as a drug delivery system. Au surface was chosen because of its chemical simplicity and inertness, as well as its modification with thiol-containing SAM has been well developed [45,46]. We fabricated MIL-88B(Fe) thin film following a SAM modification using MHDA on Au surface. Loading ibuprofen, as a model drug, was achieved by a direct soaking procedure in a non-polar organic solvent. The direct mass comparison of the film before and after loading with ibuprofen was achieved using gravimetric method, a quartz crystal microbalance (QCM), which was also applied to analyze the drug releasing profile in a static immersion condition. The surface morphology after each modification step was monitored by scanning electron microscopy (SEM). Furthermore, we investigated the surface binding mechanisms between MIL-88B(Fe) and the MHDA SAM based on the density functional theory (DFT) cluster calculations using Gaussian.

2. Material and methods

2.1. Chemicals and materials

All chemicals were reagent grade or better, used as received, and included iron chloride hexahydrate ($\text{FeCl}_3 \cdot 6 \text{ H}_2\text{O}$, Acros Organic, 99 +%), terephthalic acid (Acros Organic 99 +%), dimethylformamide (DMF, Fisher Chemical, 99.9 %), hydrogen peroxide (Fisher Chemical, 30 %), Milli-Q water (Milli-Pore, 18.2 M Ω •cm), ammonia hydroxide.

(EMD, 30 %), ibuprofen (Acros Organic, 99 %), and phosphate-buffered saline (PBS, Gibco, pH 7.2, 1x, with 0.5 % Tween20).

Gold-coated silicon wafers ($50 \pm 5 \text{ nm}$ of Au on $500 \pm 30 \mu\text{m}$ p-type Si (111), Ted Pella) and AT-cut piezoelectric quartz crystal sensors coated with Au with a resonant frequency of 5 MHz (SRS) were used in this study.

2.2. Sample preparation

2.2.1. Synthesis of MIL-88B(Fe)—MIL-88B(Fe) was synthesized following a procedure modified from literature [17,47] 0.270 g (1 mmol) of $\text{FeCl}_3 \cdot 6 \text{ H}_2\text{O}$ and 0.116 g (1 mmol) of terephthalic acid was dissolved in 5 mL of dimethylformamide (DMF) in a glass reactor, followed by adding 0.4 mL of 2.0 M NaOH and sonicating for 2 min. Reaction vials were placed in an oven at 100 °C for 12 h. The resulting MIL-88B(Fe) bulk powder was separated from its mother solution by vacuum filtration. The mother solution was further centrifuged (5000 RPM for 15 min) to separate smaller MIL-88B(Fe) solids from DMF. The pellet was then washed by three cycles of centrifugation and resuspended in ethanol. This MIL-88B(Fe) ethanol solution was used to prepare MIL-88B thin films. The

bulk MIL-88B(Fe) powder from vacuum filtration was further washed with deionized water and acetone, then dried overnight in an oven at 110 °C for later XRD and IR studies.

2.2.2. Preparation of functionalized Au—Prior to any experiment, the gold-coated silicon wafers and quartz crystal sensors were thoroughly cleaned using a standardized procedure: The gold samples were sonicated in ethanol for 5 min and placed in a UV-ozone cleaner (Bioforce Nanosciences) for 10 min. Next, they were subjected to a preheated (75 °C) 5:1:1 ratio of Milli-Q water, hydrogen peroxide, and a 30 % ammonia solution for 5 min, followed by a thorough rinsing with Milli-Q water. The samples were then placed in the UV-ozone cleaner for 10 min following drying with nitrogen. Lastly, the pre-cleaned Au samples were soaked in a MHDA ethanol solution (1 mM) for 24 h at room temperature to grow a COOH-terminated SAM.

2.2.3. Preparation of SURMOF MIL-88B thin films—A MHDA functionalized gold-coated silicon wafer was placed in the collected mother solution for 24 h at room temperature with the gold-plated side facing upwards. After direct crystallization soaking, the sample was rinsed with DMF and ethanol, followed by drying with N₂.

2.3. Drug delivery studies

2.3.1. Drug loading into MIL-88B modified gold surface—MIL-88B(Fe) coated gold surface was placed into freshly prepared 0.5 mg/mL of ibuprofen in hexane solution for 24 h for drug loading. After that, the sample was rinsed thoroughly in hexane and ethanal, respectively, to remove any outer surface adsorbed ibuprofen before drying with nitrogen. The prepared samples were then ready for surface characterization and further drug release experiments. The drug loading amount was determined by measuring the resonance frequency change of the Au sensor using a QCM after each surface modification step.

2.3.2. Drug release studies—Ibuprofen loaded MIL-88B film on an Au coated quartz sensor (5 MHz) was immersed in 60 mL PBS with 0.5 % Tween 20 solution at room temperature for varied testing time, meanwhile the frequency change of the quartz crystal was monitored in situ using a QCM. The still immersion release experiment is referred as static drug elution.

2.4. Characterization techniques

2.4.1. Powder X-ray diffraction (PXRD)—Powder X-Ray diffraction (PXRD) data was collected using a PANalytical X'pert Pro MPD diffractometer equipped with a linear X'Celerator detector and a Cu K α_1 radiation source. Diffraction data was collected at room temperature in the range of 5–40 degrees with a ~0.008 step size.

2.4.2. Attenuated total reflectance infrared spectroscopy (ATR-IR)—Attenuated total reflectance infrared (ATR-IR) spectra were collected using a Fourier transform infrared spectrometer (FTIR) with an attenuated total reflectance accessory. The spectra were collected in a range of 4000–400 cm⁻¹ with a resolution of 4 cm⁻¹ and 128 scans per measurement. Air was used as the background.

2.4.3. Quartz crystal microbalance (QCM)—Real time frequency data was collected using a QCM200 system (SRS) attached with a QCM25 crystal oscillator for 1" diameter 5 MHz AT-cut crystals for open air experiments. The crystal sensor was placed into the crystal head holder attached with a retainer cover. Five types of samples were measured, including clean Au, COOH-terminated Au, MIL-88B(Fe) coated COOH-terminated Au, and pre- and post-ibuprofen released from MIL-88B(Fe) on COOH-terminated Au. For sufficient equilibration, crystals were allowed to oscillate for at least 30 mins before taking any measurements. Data was then logged for at least an hour or until large fluctuations in data no longer occurred. To verify the mass change of the QCM Au surface after each modification step and the drug releasing properties of MIL-88B(Fe) film, raw data was analyzed using the Sauerbrey relation, [48] as described in Eq. 1.

$$\Delta f = -Cf \cdot \Delta m \quad \text{Eq. 1}$$

where f is the observed frequency change in Hz, m is the change in mass per unit area in $\mu\text{g}/\text{cm}^2$, and Cf is the sensitivity factor for the crystal ($56.6 \text{ Hz}\cdot\mu\text{g}^{-1}\cdot\text{cm}^2$ for a 5 MHz AT-cut quartz crystal at room temperature).

2.4.4. Scanning electron microscopy (SEM)—Scanning electron microscopic images were collected using a FEI Quanta 650 and a Thermo Scientific Phenom G6 Desktop SEM to study the morphology changes of MIL-88B(Fe) film on functionalized QCM Au chips after each modification. The images were taken with an acceleration voltage of between 10 and 20 kV and a working distance between 6 and 10 mm in high vacuum condition. For a better resolution, all samples were sputter-coated with gold prior to SEM imaging.

2.5. Computational details

Two possible adsorption mechanisms of MIL-88B(Fe) on a COOH-terminated Au surface were explored by cluster calculations based on the density functional theory (DFT). Additionally, full natural bonding orbital (NBO) calculations were performed to study the interactions between MIL-88B(Fe) and ibuprofen to simulate the drug loading process. All calculations were performed with the Gaussian 16 suite of programs (Rev. A.03) [49] using the B3LYP approximation to the exchange-correlated functional [50–52] with LanL2DZ basis set [53,54]. MIL-88B(Fe) is represented by a cluster model of $\text{C}_6\text{H}_{15}\text{O}_{16}$, as shown in Fig. S1, which was achieved using a cluster extraction method in which a fraction or truncated form of the extended solid (framework) is treated with high level of computational theory [55]. All molecular structures in this study were constructed using IQmol, a free open-source molecular editor and visualization package. Then, these structures were transferred to and visualized in GuassView 6 (Rev 6.0.16). Geometrical optimizations were performed on all relevant structures of MIL-88B(Fe), ibuprofen, acetic acid which simulates the functional end group of a COOH-terminated SAM. The optimized molecular geometries were verified to be minima by calculating the vibrational frequencies and finding no imaginary frequencies. The reported electronic energies of each resulting structures were then used to calculate the optimal energy for the two competing mechanistic models using a derivative of Hess's Law (Eq. 2).

$$\Delta E_{reaction} = \sum \Delta E_{products} - \sum \Delta E_{reactants} \quad \text{Eq. 2}$$

where $E_{reaction}$ is the change of energy between products and reactants, $\Sigma E_{products}$ is the sum of the energy of all products after optimization, and $\Sigma E_{reactants}$ is the sum of the energy of all reactants after optimization.

3. Results and discussions

3.1. Characterization of surface supportive MIL-88B(Fe) film

After solvothermal synthesis, MIL-88B(Fe) went through a solvent exchange process with 200 proof ethanol to remove any residue DMF trapped in the pores. The bulk MIL-88B(Fe) crystal structure was confirmed by comparing the PXRD patterns (Fig. 1) with the simulated diffraction diagram and the previously reported diffraction patterns in literature [56,57]. After confirming the correct material, we used the MIL-88B(Fe) ethanol solution to prepare films on functionalized Au substrates. The surface modification steps are illustrated in Scheme 1. We started with a clean gold-coated silicon wafer obtained via an established chemical and UV/ozone cleaning method.[58] The gold surface was then functionalized with MHDA to form a COOH-terminated SAM. The formation of SAM was confirmed by the IR spectrum (Fig. 2b), as indicated by the C-H symmetric and asymmetric stretch shown at 2927 and 2854 cm⁻¹ and the C=O stretch from the carboxylic acid groups at 1739 cm⁻¹ [59,60]. After soaking in the MIL-88B(Fe) ethanol solution for a predetermined time period, the MHDA-modified Au surface was covered with MIL-88B(Fe) crystals, confirmed by the XRD result by comparing with its bulk powder pattern. Additionally, the chemical composition of MIL-88B(Fe) film was studied using ATR-IR. Fig. 2c exhibits two sharp and well-defined peaks at 1392 and 1599 cm⁻¹ corresponding to the symmetric and asymmetric vibrations of carboxylate (O-C=O) stretching from MIL-88B.[19] The aromatic C-H stretch from the terephthalate ligands was observed as a broad band at 3100 cm⁻¹. The Fe-O stretch from the trimeric FeO₆ octahedral clusters was observed at 556 cm⁻¹.[61] These observations confirmed the formation of MIL-88B on the COOH-functionalized Au surface. The strong C=O stretching peak at 1599 cm⁻¹ was not related to the carbonyl groups from DMF as no obvious C-H stretching peaks were observed in the region of 2800 – 3000 cm⁻¹, moreover, we conducted a solvent exchange on MIL-88B to replace the DMF synthesis solution. Combining the XRD and ATR-IR studies, we confirmed the crystal structure and chemical composition of MIL-88B(Fe) attached to the surface of a modified Au surface. The surface morphology was further examined using SEM. Fig. 3a shows a clean gold coated silicon wafer with a flat and intact surface free of debris before modification steps. After being treated with MIL-88B(Fe) ethanol solution, the SAM-modified Au surface was covered with MIL-88B(Fe) crystals as observed in Fig. 3b. The SEM image of surface-supported MIL-88B(Fe) shows a characteristic “rice-grain” shape of these crystals with a size of ~500 nm along the c-axis, which is consistent with previous studies [16, 43] Although the resulting MIL-88B(Fe) film was prepared using a solvent-exchanged mother solution, the shape of crystals did not change compared to the bulk MIL-88B(Fe) that was synthesized through a solvothermal method with DMF. The surface was covered with MIL-88B (Fe) crystals. We attribute it to the carboxylate

Author Manuscript
Author Manuscript
Author Manuscript
Author Manuscript

end groups of the MHDA facilitate the growth of MIL-88B(Fe). The morphology studies provided evidence that the MIL-88B(Fe) crystals remain intact during the mother solution immersion process and were attached to the functionalized Au surface as expected. The amount of MIL-88B(Fe) adsorbed on surface was examined using a QCM and will be discussed in the following section. After confirming the film of MIL-88B(Fe) was built on top of the modified Au surface, we performed drug loading and elution studies on these films.

3.2. Study of drug loading and releasing of MIL-88B(Fe) film

Ibuprofen, a nonsteroidal anti-inflammatory drug, was chosen as the model drug for this study due to the following reasons: First, its molecular size ($4 \times 6 \times 10 \text{ \AA}$) is compatible with the pore entrance of MIL-88B(Fe) framework ($9.5 \times 19.0 \text{ \AA}$);[19] Second, ibuprofen has unique vibrational frequency and XRD patterns that are different from MIL-88B (Fe) which makes it an excellent candidate for characterization; Lastly and most importantly, ibuprofen's intrinsic hydrophobic nature establishes predictable strong interactions with the inter-pores of MIL-88B (Fe).[16] Based on ibuprofen's hydrophobicity, hexane was selected as the solvent for drug encapsulation process due to the high solubility of ibuprofen in hexane. Prior to the drug loading experiments, we tested the stability of MIL-88B(Fe) film in hexane. Our XRD studies confirmed the film remained its crystalline structure after 24 hr soaking. We immersed the MIL-88B(Fe) film coated Au sample in the ibuprofen/hexane solution (0.5 mg/mL) for 24 h, then rinsed the surface with pure hexane to remove surface adsorbed residual ibuprofen. After that, the surface was rinsed with ethanol thoroughly to remove any hexane residue. To verify if the ibuprofen was incorporated into the MIL-88B (Fe) film, ATR-IR spectrum was taken after the drug loading experiment. From the IR results (Fig. 2d), we noticed the vibration of C=O stretch at 1600 cm^{-1} was greatly enhanced after the surface was treated with ibuprofen/hexane solution. Additionally, the symmetric/asymmetric C-H stretching features were observed at 2923 and 2870 cm^{-1} . These observations confirm that ibuprofen has been encapsulated inside of the MIL-88B(Fe) film. To ensure no surface adsorbed ibuprofen or hexane left, all tested samples were rinsed with ethanol and dried with nitrogen before performing IR measurements. The SEM image shown in Fig. 3c reveal that the morphology of MIL-88B(Fe) crystals remain intact after loading with ibuprofen. The chemical composition of MIL-88B(Fe) was not altered either, as confirmed by the IR study shown in Fig. 2d; all major vibration peaks from MIL-88B(Fe) were not shifted.

To further estimate the drug loading capacity, we performed QCM analysis to measure mass changes corresponding to each modification step. We used the Sauerbrey equation (Eq.1) to calculate mass changes based on the measured frequency differences. Fig. 4 summarizes the increasing mass of a clean Au coated quartz sensor after being modified with MHDA, MIL-88B(Fe), and ibuprofen loading. We noticed that the mass of the Au sensor had increased following functionalization with the COOH-terminated SAM, as shown in Fig. 4. The observed QCM frequency indicates $0.824 \pm 0.001 \mu\text{g/cm}^2$ of MHDA layer was built on the clean Au surface, followed by $17.103 \pm 0.021 \mu\text{g/cm}^2$ of MIL-88B(Fe) film achieved after the direct crystallization. After loading with ibuprofen, the adsorbed mass of the modified quartz crystal was found to be $1.481 \pm 0.001 \mu\text{g/cm}^2$, indicating an

encapsulation of 8.7 wt % of ibuprofen by MIL-88B. This value is markedly smaller than the drug loading capacity of bulk MIL-88B(Fe) material (~19.6 wt%).[16] We believe the lower drug loading percentage was due to the nanostructure of MIL-88B(Fe) crystals and their orientation on the supportive substrate which limited the accessible surface area for the diffusion of drug molecules. Despite a decrease in loading capacity in comparison to bulk MIL-88B(Fe), our MIL-88B(Fe) thin film still exceeds the performance compared to traditional polymer-based drug-loading films (usually with a value of ~5 %).[62].

In addition, we performed QCM studies during the drug eluting process in a static setting. PBS was used as a medium to mimic drug releasing in a physiologic environment.[63] 0.5 % of Tween 20 in volume was added to the PBS solution to increase the solubility of ibuprofen in the testing media. We noticed that the mass change was approximately 2 $\mu\text{g}/\text{cm}^2$ after 6 hr, shown in Fig. 5. The amount of ibuprofen released is consistent with the ibuprofen loading amount measured using QCM. The measured mass decrease can be resulted from both ibuprofen release and the degradation of MIL-88B(Fe) in PBS. Based on our previous study, ibuprofen releasing from MIL-88B(Fe) can be through three approaches: diffusion, surface erosion and bulk erosion of the MIL.[16] The surface morphology of the tested QCM sensor was examined using SEM after the elution experiment, as shown in Fig. 3d. The existence of MIL-88B(Fe) crystals is consistent with our QCM study, confirming some MIL-88B(Fe) remained on the surface after releasing ibuprofen. However, the morphology of these MIL-88B(Fe) crystals had changed dramatically characterized by a less dense surface coverage, as shown in Fig. 3d. This confirms the drug releasing was partially due to the degradation of MIL-88B(Fe) soaking in PBS solution. Previous studies from Serre's group have shown that the degradation of Fe-MILs in a simulated body fluid can take up to 21 days.[24] In our case, the lifetime of MIL-88B(Fe) was noticed shorter than the reported value. We suspect that the MHDA SAM may be more susceptible to the PBS solution, thus affect the MIL-88B(Fe) film on top. Besides the static drug elution study performed using QCM, the quantification of ibuprofen releasing in PBS was attempted with a high performance liquid chromatography (HPLC). However, due to the low concentration (< 70 ng/mL), we could not obtain quantitative results to confirm the ratio between ibuprofen released and MIL-88B degradation that caused the mass decrease.

3.3. Mechanistic exploration of surface-supported MIL-88B(Fe) and ibuprofen loading

Fig. 6 illustrates two general reaction pathways for MIL-88B(Fe) bonding to a COOH-terminated Au surface. Basically, the interactions of MIL-88B(Fe) and carboxylate functional groups from the SAM can be attributed to 1) hydrogen-bonding between terephthalate organic ligands and carboxylate end groups from the SAM, referring to Model A shown in Fig. 6; and 2) unsaturated Fe trimer making coordination bond with oxygen in the deprotonated carboxylate group, referring to Model B. Here, we used a well-known cluster extraction method to create a MIL-88B(Fe) cluster to represent the whole framework. This is an efficient and advantageous method in computational modeling of MOFs as there is a decrease in computational complexity due to a reduction in the number of electronic in the simulated system. Further use of cluster extraction methodology is noted to provide a unique approach that significantly improved electronic convergence that are especially importantly for MOF structures that contains strained geometries due to the presence of

Author Manuscript
Author Manuscript
Author Manuscript
Author Manuscript

metal clusters.[55] From the frontier orbital analysis, we noticed that both unsaturated Fe center and the -OH group from the end terephthalate molecule can be engaged in bonding to the MHDA SAM. Geometrical optimizations afforded the energetic information about each relevant molecular structure. The formation of hydrogen bonding (Model A) gains – 72.46 kJ/mol and for bonding to the unsaturated Fe site (Model B) this number is – 592.24 kJ/mol. Although both pathways seem feasible, model B is thermodynamically more favorable. The data in Table S1 summarizes this information for all products and reactants, and showcases E (calculated based on Eq. 2) for each of the two competing mechanistic models. All input file data is provided in Supplemental Information. To ensure that the correct structures were used to solve for E , the total number of atoms were counted to ensure that the change is zero. Since the formation of model B is energetically more favorable, we performed a detailed DFT computational study of its corresponding reaction pathway.

In order to study the interactions between MIL-88B(Fe) and ibuprofen, we performed full natural bond orbital (NBO) analysis on ibuprofen and MIL-88B(Fe) represented by the same Fe cluster used in our reaction pathway calculations. Fig. 7 compares the highest occupied molecular orbitals (HOMOs) and lowest unoccupied molecular orbitals (LUMOs) of MIL-88B(Fe) and ibuprofen. In the frontier orbital analysis, the HOMO and LUMO of ibuprofen are delocalized over the phenyl ring; while the HOMO and LUMO of MIL-88B(Fe) are primarily localized on the oxygen atoms near the saturated Fe sites which are further connected with terephthalate ligands, indicating a π -CH interaction between ibuprofen and MIL-88B(Fe). This is consistent with previously reported interactions between ibuprofen and MIL-53(Fe) simulated with DFT periodic calculations.[24] We also included a terephthalate ligand in the MIL-88B(Fe) cluster for comparison in our NBO calculations, illustrated in Fig. S2, the HOMO and LUMO were not changed. Moreover, the interactions between ibuprofen and MIL-88B(Fe) can also include the hydrogen bonding between carboxylic group in ibuprofen and hydroxyl in MIL-88B(Fe), as well as the π - π interaction between the phenyl group in ibuprofen and terephthalate in MIL-88B(Fe). All of these arrangements could be the driving force for ibuprofen loading into the cages of MIL-88B(Fe).

4. Conclusions

In this study, we successfully prepared MIL-88B(Fe) film on a COOH-terminated SAM coated Au substrate as a drug delivery system for loading and releasing ibuprofen. We confirmed the surface supportive MIL-88B(Fe) film was coordinated with carboxylate groups from the functional groups of the SAM. The drug loading capacity for such MIL-88B(Fe) film was about 8.7 % with ibuprofen. This value is greater than other polymer-based thin film drug delivery systems. Our study compared two competing mechanistic models to better understand the chemical and physical nuances of binding between MIL-88B(Fe) and the carboxylic end of MHDA. Although both hydrogen-bonding and open-metal sites are feasible for bonding, unsaturated metal sites for coordination was found thermodynamically more favorable based on our DFT cluster simulations. Furthermore, DFT calculations indicated a strong interaction between ibuprofen and the Fe-trimmers within the MIL-88B (Fe) structure which facilitates the drug loading process. Drug elution was evaluated in static condition with the aid of QCM. We quantified the drug releasing amount

as a function of time and identified the drug releasing mechanism was due to both drug molecule diffusion and material degradation. Overall, MIL-88B(Fe) has exhibited excellent potential to be used as a drug delivery system considering its high drug loading capacity, biodegradation properties, and overall versatility.

Supplementary Material

Refer to Web version on PubMed Central for supplementary material.

Funding

Research reported in this publication was supported by the National Institute of General Medical Sciences of the National Institutes of Health, USA under Award Number SC3GM136590. The content is solely the responsibility of the authors and does not necessarily represent the official views of the National Institutes of Health. This work was also partially supported by the California State University Long Beach RSCA Award.

Data Availability

Data will be made available on request.

References

- [1]. Lee J, Farha OK, Roberts J, Scheidt KA, Nguyen ST, Hupp JT, Metal–organic framework materials as catalysts, *Chem. Soc. Rev.* 38 (2009) 1450, 10.1039/b807080f. [PubMed: 19384447]
- [2]. Liu J, Wöll C, Ma LQ, Papanikolas JM, Meyer TJ, Lin WB, Wilmer CE, Sarjeant AA, Schatz GC, Snurr RQ, Farha OK, Wiederrecht GP, Hupp JT, Serre C, Ma J, Loo SCJ, Wei WD, Yang YH, Hupp JT, Huo FW, Smit B, Kortright JB, Gagliardi L, Bordiga S, Reimer JA, Long JR, Surface-supported metal–organic framework thin films: fabrication methods, applications, and challenges, *Chem. Soc. Rev.* 417 (2017) 813–821, 10.1039/C7CS00315C.
- [3]. Shekhh O, Liu J, Fischer RA, Wöll C, MOF thin films: existing and future applications, *Chem. Soc. Rev.* 40 (2011) 1081–1106, 10.1039/c0cs00147c. [PubMed: 21225034]
- [4]. Spokoyny AM, Kim D, Sumrein A, Mirkin CA, Infinite coordination polymer nano- and microparticle structures, *Chem. Soc. Rev.* 38 (2009) 1218, 10.1039/b807085g. [PubMed: 19384433]
- [5]. Millward AR, Yaghi OM, Metal-organic frameworks with exceptionally high capacity for storage of carbon dioxide at room temperature, *J. Am. Chem. Soc.* 127 (2005) 17998–17999, 10.1021/ja0570032. [PubMed: 16366539]
- [6]. Li J-R, Kuppler RJ, Zhou H-C, Selective gas adsorption and separation in metal-organic frameworks, *Chem. Soc. Rev.* 38 (2009) 1477–1504, 10.1039/b802426j. [PubMed: 19384449]
- [7]. Chin M, Cisneros C, Araiza SM, Vargas KM, Ishihara KM, Tian F, Rhodamine B degradation by nanosized zeolitic imidazolate framework-8 (ZIF-8), *RSC Adv.* 8 (2018) 26987–26997, 10.1039/C8RA03459A. [PubMed: 30174827]
- [8]. Lin J-B, Nguyen TTT, Vaidhyanathan R, Burner J, Taylor JM, Durekova H, Akhtar F, Mah RK, Ghaffari-Nik O, Marx S, Fylstra N, Iremonger SS, Dawson KW, Sarkar P, Hovington P, Rajendran A, Woo TK, Shimizu GKH, A scalable metal-organic framework as a durable physisorbent for carbon dioxide capture, *Science* 374 (2021) 1464–1469, 10.1126/SCIENCE.ABI7281. [PubMed: 34914501]
- [9]. Mon M, Bruno R, Ferrando-Soria J, Armentano D, Pardo E, Metal–organic framework technologies for water remediation: towards a sustainable ecosystem, *J. Mater. Chem. A* 6 (2018) 4912–4947, 10.1039/C8TA00264A.
- [10]. Khan S, Guan Q, Liu Q, Qin Z, Rasheed B, Liang X, Yang X, Synthesis, modifications and applications of MILs Metal-organic frameworks for environmental remediation: the cutting-edge

- review, *Sci. Total Environ.* 810 (2022), 152279, 10.1016/J.SCITOTENV.2021.152279. [PubMed: 34902423]
- [11]. Jiang C, Wang X, Ouyang Y, Lu K, Jiang W, Xu H, Wei X, Wang Z, Dai F, Sun D, Recent advances in metal–organic frameworks for gas adsorption/separation, *Nanoscale Adv.* (2022), 10.1039/D2NA00061J.
- [12]. Lawson HD, Walton SP, Chan C, Metal–organic frameworks for drug delivery: a design perspective, *ACS Appl. Mater. Interfaces* 13 (2021) 7004–7020. [PubMed: 33554591]
- [13]. Nanostructured metal–organic frameworks and their bio-related applications, in: Giménez-Marqués M, Hidalgo T, Serre C, Horcajada P (Eds.), *Coord. Chem. Rev.* 307, 2015, pp. 342–360, 10.1016/j.ccr.2015.08.008.
- [14]. Horcajada P, Chalati T, Serre C, Gillet B, Sebrie C, Baati T, Eubank JF, Heurtaux D, Clayette P, Kreuz C, Chang J-S, Hwang YK, Marsaud V, Bories P-NN, Cynober L, Gil S, Férey G, Couvreur P, Gref R, Porous metal–organic-framework nanoscale carriers as a potential platform for drug delivery and imaging, *Nat. Mater.* 9 (2010) 172–178, 10.1038/nmat2608. [PubMed: 20010827]
- [15]. Della Rocca J, Liu D, Lin W, Nanoscale metal–organic frameworks for biomedical imaging and drug delivery, *Acc. Chem. Res.* 44 (2011) 957–968, 10.1021/ar200028a. [PubMed: 21648429]
- [16]. Pham H, Ramos K, Sua A, Acuna J, Slowinska K, Nguyen T, Bui A, Weber MDR, Tian F, Tuning crystal structures of iron-based metal–organic frameworks for drug delivery applications, *ACS Omega* 5 (2020) 3418–3427, 10.1021/acsomega.9b03696. [PubMed: 32118156]
- [17]. Surblé S, Serre C, Mellot-Draznieks C, Millange F, Férey G, A new isoreticular class of metal–organic-frameworks with the MIL-88 topology, *Chem. Commun.* (2006) 284–286, 10.1039/b512169h.
- [18]. Serre C, Millange F, Surblé S, Férey G, A route to the synthesis of trivalent transition-metal porous carboxylates with trimeric secondary building units, *Angew. Chem. Int. Ed.* 43 (2004) 6285–6289, 10.1002/anie.200454250.
- [19]. Horcajada P, Salles F, Wuttke S, Devic T, Heurtaux D, Maurin G, Vimont A, Daturi M, David O, Magnier E, Stock N, Filinchuk Y, Popov D, Riekel C, Férey G, Serre C, How linker’s modification controls swelling properties of highly flexible iron(III) dicarboxylates MIL-88, *J. Am. Chem. Soc.* 133 (2011) 17839–17847, 10.1021/ja206936e. [PubMed: 21950795]
- [20]. McKinlay AC, Morris RE, Horcajada P, Férey G, Gref R, Couvreur P, Serre C, BioMOFs: metal–organic frameworks for biological and medical applications, *Angew. Chem. Int. Ed.* 49 (2010) 6260–6266, 10.1002/anie.201000048.
- [21]. Xiao Y, Guo X, Huang H, Yang Q, Huang A, Zhong C, Synthesis of MIL-88B(Fe)/Matrimid mixed-matrix membranes with high hydrogen permselectivity, *RSC Adv.* 5 (2015) 7253–7259, 10.1039/C4RA13727B.
- [22]. McKinlay AC, Eubank JF, Wuttke S, Xiao B, Wheatley PS, Bazin P, Lavalley J-C, Daturi M, Vimont A, De Weireld G, Horcajada P, Serre C, Morris RE, Nitric oxide adsorption and delivery in flexible MIL-88(Fe) metal–organic frameworks, *Chem. Mater.* 25 (2013) 1592–1599, 10.1021/cm304037x
- [23]. Horcajada P, Serre C, Vallet-Regí M, Sebban M, Taulelle F, Férey G, Metal–organic frameworks as efficient materials for drug delivery, *Angew. Chem. Int. Ed. Engl.* 45 (2006) 5974–5978, 10.1002/anie.200601878. [PubMed: 16897793]
- [24]. Horcajada P, Serre C, Maurin G, Ramsahye NA, Balas F, Vallet-Regí M, Sebban M, Taulelle F, Férey G, Flexible porous metal–organic frameworks for a controlled drug delivery, *J. Am. Chem. Soc.* 130 (2008) 6774–6780, 10.1021/ja710973k. [PubMed: 18454528]
- [25]. Devic T, Horcajada P, Serre C, Salles F, Maurin G, Moulin B, Heurtaux D, Clet G, Vimont A, Grenéche JM, Le Ouay B, Moreau F, Magnier E, Filinchuk Y, Marrot J, Lavalley JC, Daturi M, Férey G, Functionalization in flexible porous solids: effects on the pore opening and the host-guest interactions, *J. Am. Chem. Soc.* 132 (2010) 1127–1136, 10.1021/ja9092715. [PubMed: 20038143]
- [26]. Zhuang J, Kuo C-H, Chou L-Y, Liu D-Y, Weerapana E, Tsung C-K, Optimized metal–organic-framework nanospheres for drug delivery: evaluation of small-molecule encapsulation, *ACS Nano* 8 (2014) 2812–2819, 10.1021/nn406590q. [PubMed: 24506773]

- [27]. Tamames-Tabar C, Cunha D, Imbuluzqueta E, Ragon F, Serre C, Blanco-Prieto MJ, Horcajada P, Cytotoxicity of nanoscaled metal–organic frameworks, *J. Mater. Chem. B* 2 (2014) 262–271, 10.1039/C3TB20832J. [PubMed: 32261505]
- [28]. Chen W, Habraken TCJ, Hennink WE, Kok RJ, Polymer-free drug-eluting stents: an overview of coating strategies and comparison with polymer-coated drug-eluting stents, *Bioconjug. Chem* 26 (2015) 1277–1288, 10.1021/acs.bioconjchem.5b00192. [PubMed: 26041505]
- [29]. Khan W, Farah S, Domb AJ, Drug eluting stents: developments and current status. *J. Control. Release* 161 (2012) 703–712, 10.1016/j.jconrel.2012.02.010. [PubMed: 22366546]
- [30]. Liu B, Shekhah O, Arslan HK, Liu J, Wöll C, Fischer RA, Enantiopure metal–organic framework thin films: oriented SURMOF growth and enantioselective adsorption, *Angew. Chem. Int. Ed* 51 (2012) 807–810, 10.1002/anie.201104240.
- [31]. Heinke L, Tu M, Wannapaiboon S, Fischer RA, Wöll C, Surface-mounted metal–organic frameworks for applications in sensing and separation, *Microporous Mesoporous Mater.* 216 (2015) 200–215, 10.1016/j.micromeso.2015.03.018.
- [32]. Ruiz MA, Sua A, Tian F, Covalent attachment of metal–organic framework thin films on surfaces, *Encycl. Interfacial Chem. Surf. Sci. Electrochem* 4 (2018) 646–671, 10.1016/B978-0-12-409547-2.14124-1.
- [33]. Wang Z, Yan Y, Controlling crystal orientation in zeolite MFI thin films by direct in situ crystallization, *Chem. Mater* 13 (2001) 1101–1107, 10.1021/cm000849e.
- [34]. Bétard A, Fischer RA, Metal–organic framework thin films: from fundamentals to applications, *Chem. Rev* 112 (2012) 1055–1083, 10.1021/cr200167v. [PubMed: 21928861]
- [35]. Zacher D, Schmid R, Wöll C, a Fischer R, Surface chemistry of metal–organic frameworks at the liquid-solid interface, in: Chemie- Angew (Ed.), Int, 50, 2011, pp. 176–199, 10.1002/anie.201002451.
- [36]. Sumby CJ, Metal–organic frameworks: a thin film opening. *Nat. Chem* 8 (2016) 294–296, 10.1038/nchem.2481. [PubMed: 27001723]
- [37]. Liu J, Shekhah O, Stammer X, Arslan HK, Liu B, Schüpbach B, Terfort A, Wöll C, Deposition of Metal–organic Frameworks by Liquid-Phase Epitaxy: The Influence of Substrate Functional Group Density on Film Orientation, in: Materials, 5, Basel, 2012, pp. 1581–1592, 10.3390/ma5091581.
- [38]. Shekhah O, Eddaoudi M, The liquid phase epitaxy method for the construction of oriented ZIF-8 thin films with controlled growth on functionalized surfaces, *Chem. Commun* 49 (2013) 10079–10081, 10.1039/c3cc45343j.
- [39]. Munuera C, Shekhah O, Wang H, Wöll C, Ocal C, Kaskel S, Woll C, Evers F, Zacher D, Fischer RA, Woll C, The controlled growth of oriented metal–organic frameworks on functionalized surfaces as followed by scanning force microscopy, *Phys. Chem. Chem. Phys* 10 (2008) 7257, 10.1039/b811010g. [PubMed: 19060970]
- [40]. Zhuang J-L, Kind M, Grytz CM, Farr F, Diefenbach M, Tussupbayev S, Holthausen MC, Terfort A, Insight into the oriented growth of surface-attached metal–organic frameworks: surface functionality, deposition temperature, and first layer order, *J. Am. Chem. Soc* 137 (2015) 8237–8243, 10.1021/jacs.5b03948. [PubMed: 26051709]
- [41]. Tu M, a Fischer R, Heteroepitaxial growth of surface mounted metal–organic framework thin films with hybrid adsorption functionality, *J. Mater. Chem. A* 2 (2014) 2018, 10.1039/c3ta13812g.
- [42]. Scherb C, Schödel A, Bein T, Directing the structure of metal–organic frameworks by oriented surface growth on an organic monolayer, *Angew. Chem. Int. Ed. Engl* 47 (2008) 5777–5779, 10.1002/anie.200704034. [PubMed: 18604800]
- [43]. Scherb C, Koehn R, Bein T, Sorption behavior of an oriented surface-grown MOF-film studied by in situ X-ray diffraction, *J. Mater. Chem* 20 (2010) 3046, 10.1039/b916953a.
- [44]. Filippouli M, Turner S, Leus K, Siafaka PI, Tseligka ED, Vandichel M, Nanaki SG, Vizirianakis IS, Bikaris DN, Van Der Voort P, Van Tendeloo G, Biocompatible Zr-based nanoscale MOFs coated with modified poly (ε-caprolactone) as anticancer drug carriers, *Int. J. Pharm* 509 (2016) 208–218, 10.1016/J.IJPHARM.2016.05.048. [PubMed: 27235556]

- [45]. Tour JM, Jones L, Pearson DL, Lamba JJS, Burgin TP, Whitesides GM, Allara DL, Parikh AN, Atre S, Self-assembled monolayers and multilayers of conjugated thiols, alpha.,omega.-dithiols, and thioacetyl-containing adsorbates, understanding attachments between potential molecular wires and gold surfaces, *J. Am. Chem. Soc* 117 (1995) 9529–9534, 10.1021/ja00142a021.
- [46]. Jadhav SA, Self-assembled monolayers (SAMs) of carboxylic acids: an overview, *Cent. Eur. J. Chem* 9 (2011) 369–378, 10.2478/s11532-011-0024-8.
- [47]. Ma M, Noei H, Mienert B, Niesel J, Bill E, Muhler M, Fischer RA, Wang Y, Schatzschneider U, Metzler-Nolte N, Iron metal-organic frameworks MIL-88B and NH₂-MIL-88B for the loading and delivery of the gasotransmitter carbon monoxide, *Chem. - A Eur. J* 19 (2013) 6785–6790, 10.1002/chem.201201743.
- [48]. Rodahl M, Kasemo B, On the measurement of thin liquid overlayers with the quartz-crystal microbalance, *Sens. Actuators A Phys* 54 (1996) 448–456, 10.1016/S0924-4247(97)80002-7.
- [49]. Frisch MJ, Trucks GW, Schlegel HB, Scuseria GE, Robb MA, Cheeseman JR, Scalmani G, Barone V, Petersson GA, Nakatsuji H, Li X, Caricato M, Marenich AV, Bloino J, Janesko BG, Gomperts R, Mennucci B, Hratchian HP, Ortiz JV, Izmaylov AF, Sonnenberg JL, Williams-Young D, Ding F, Lipparini F, Egidi F, Goings J, Peng B, Petrone A, Henderson T, Ranasinghe D, Zakrzewski VG, Gao J, Rega N, Zheng G, Liang W, Hada M, Ehara M, Toyota K, Fukuda R, Hasegawa J, Ishida M, Nakajima T, Honda Y, Kitao O, Nakai H, Vreven T, Throssell K, Montgomery J, A J, Peralta JE, Ogliaro F, Bearpark MJ, Heyd JJ, Brothers EN, Kudin KN, Staroverov VN, Keith TA, Kobayashi R, Normand J, Raghavachari K, Rendell AP, Burant JC, Iyengar SS, Tomasi J, Cossi M, Millam JM, Klene M, Adamo C, Cammi R, Ochterski JW, Martin RL, Morokuma K, Farkas O, Foresman JB, Fox DJ, Gaussian, 16, 2016.
- [50]. Becke AD, A new mixing of Hartree-Fock and local density-functional theories, *J. Chem. Phys* 98 (1993) 1372–1377, 10.1063/1.464304.
- [51]. Krishnan R, Binkley JS, Seeger R, Pople JA, Self-consistent molecular orbital methods. XX. A basis set for correlated wave functions, *J. Chem. Phys* 72 (1980) 650–654, 10.1063/1.438955.
- [52]. Lee C, Yang W, Parr RG, Development of the Colle-Salvetti correlation-energy formula into a functional of the electron density, *Phys. Rev. B* 37 (1988) 785–789, 10.1103/PhysRevB.37.785.
- [53]. Martin JML, Sundermann A, Correlation consistent valence basis sets for use with the Stuttgart-Dresden-Bonn relativistic effective core potentials: the atoms Ga–Kr and In–Xe, *J. Chem. Phys* 114 (2001) 3408–3420, 10.1063/1.1337864.
- [54]. Feller D, Peterson KA, de Jong WA, Dixon DA, Performance of coupled cluster theory in thermochemical calculations of small halogenated compounds, *J. Chem. Phys* 118 (2003) 3510–3522, 10.1063/1.1532314.
- [55]. Mancuso JL, Mroz AM, Le KN, Hendon CH, Electronic structure modeling of metal-organic frameworks, *Chem. Rev* 120 (2020) 8641–8715, 10.1021/acs.chemrev.0c00148. [PubMed: 32672939]
- [56]. Xu B, Yang H, Cai Y, Yang H, Li C, Preparation and photocatalytic property of spindle-like MIL-88B(Fe) nanoparticles, *Inorg. Chem. Commun* 67 (2016) 29–31, 10.1016/J.INOCHE.2016.03.003.
- [57]. Shi L, Wang T, Zhang H, Chang K, Meng X, Liu H, Ye J, An amine-functionalized Iron(III) metal-organic framework as efficient visible-light photocatalyst for Cr(VI) reduction, *Adv. Sci* 2 (2015) 1500006, 10.1002/advs.201500006.
- [58]. Vig JR, U.V. Ozone, cleaning of surfaces, *J. Vac. Sci. Technol. A Vac. Surf. Film* 3 (1985) 1027, 10.1116/1.573115.
- [59]. Thamri A, Baccar H, Struzzi C, Bittencourt C, Abdelghani A, Llobet E, MHDA-functionalized multiwall carbon nanotubes for detecting non-aromatic VOCs, *Sci. Rep* 6 (2016), 10.1038/srep35130.
- [60]. Roussille L, Brotons G, Ballut L, Louarn G, Ausserré D, Ricard-Blum S, Surface characterization and efficiency of a matrix-free and flat carboxylated gold sensor chip for surface plasmon resonance (SPR), *Anal. Bioanal. Chem* 401 (2011) 1605–1621, 10.1007/s00216-011-5220-z.
- [61]. Yi X, He X, Yin F, Yang T, Chen B, Li G, NH₂-MIL-88B-Fe for electrocatalytic N₂ fixation to NH₃ with high Faradaic efficiency under ambient conditions in neutral electrolyte, *J. Mater. Sci* 55 (2020) 12041–12052, 10.1007/S10853-020-04777-2/FIGURES/4.

- [62]. Huang W, Tsui CP, Tang CY, Gu L, Effects of compositional tailoring on drug delivery behaviours of silica xerogel/polymer core-shell composite nanoparticles, *Sci. Rep.* 8 (2018) 13002, 10.1038/s41598-018-31070-9. [PubMed: 30158709]
- [63]. Miller SR, Heurtaux D, Baati T, Horcajada P, Grenèche J-M, Serre C, Biodegradable therapeutic MOFs for the delivery of bioactive molecules, *Chem. Commun.* 46 (2010) 4526–4528, 10.1039/c001181a.

Author Manuscript

Author Manuscript

Author Manuscript

Author Manuscript

HIGHLIGHTS

- Metal-organic framework thin film can be fabricated on a desired substrate.
- MIL-88B(Fe) thin film can be used for potential drug elution coating.
- A sustainable drug release behavior was observed for MIL-88B(Fe) thin films.
- Unsaturated metal site plays an important role on binding to modified substrate.

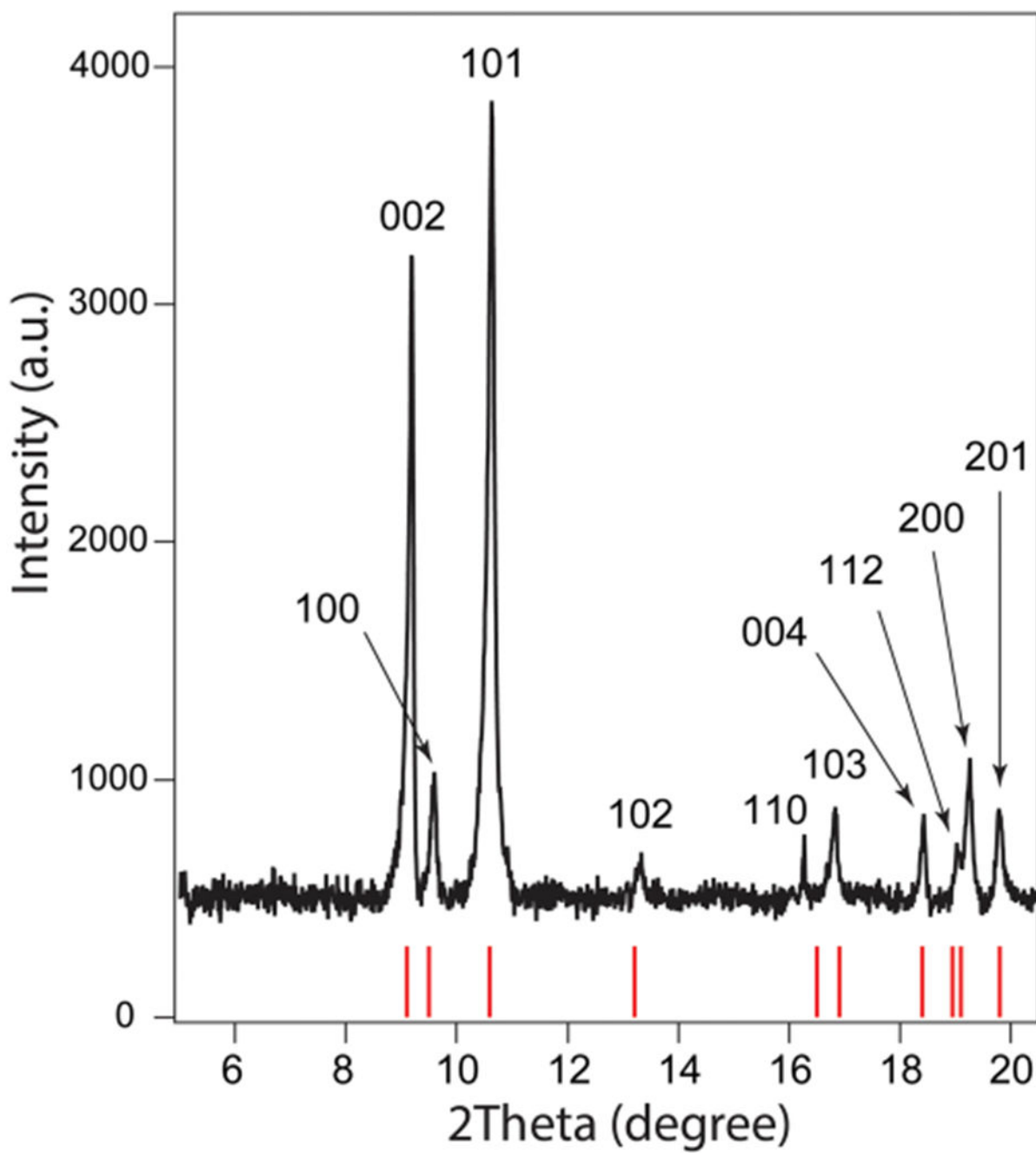


Fig. 1.
PXRD pattern of bulk MIL-88B(Fe) powder compared with simulated patterns (solid bars).

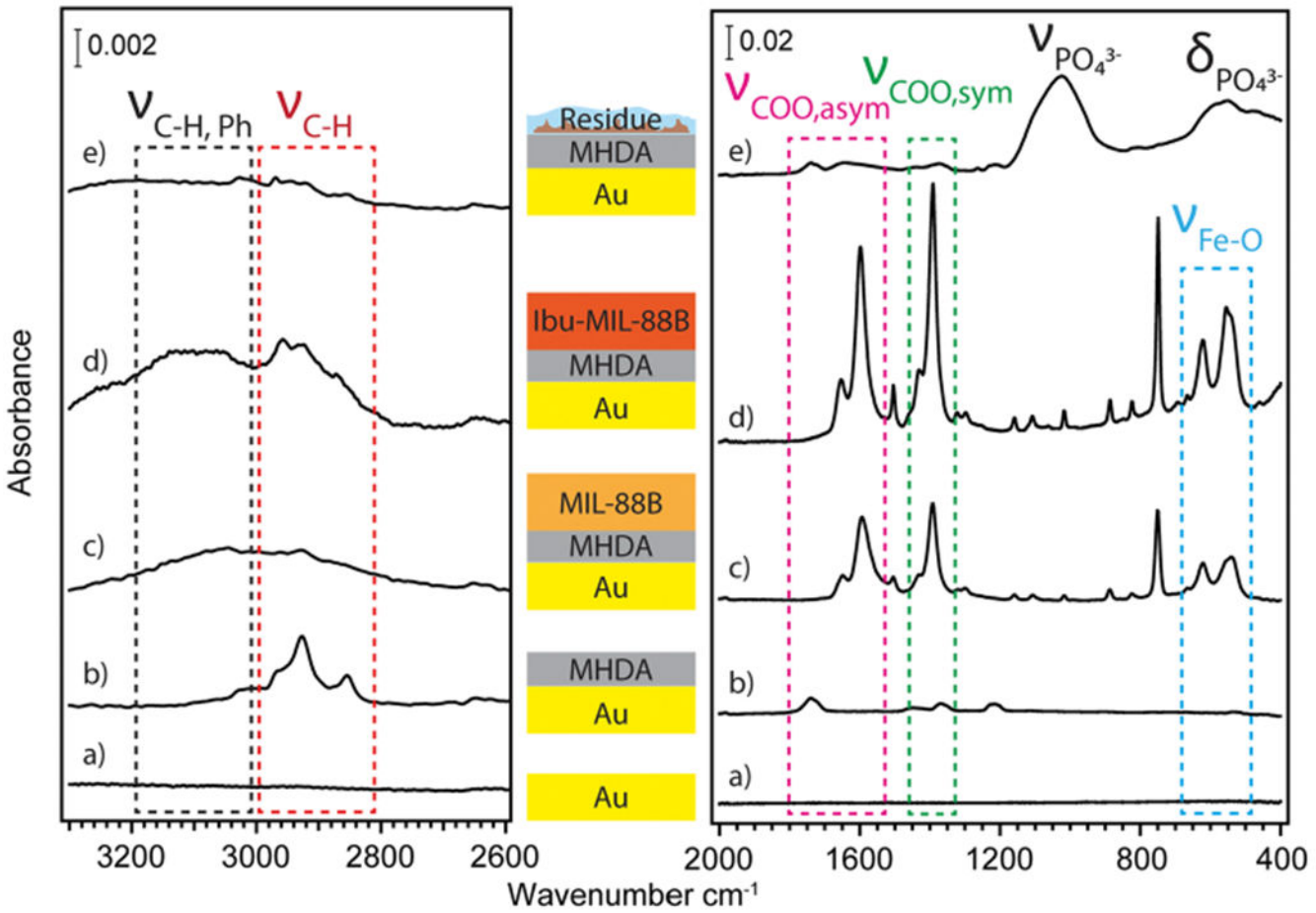


Fig. 2.
ATR-IR spectra of a) clean Au surface, b) MHDA SAM modified Au surface, c) MIL-88B(Fe) thin film on a MHDA-functionalized Au substrate, d) ibuprofen loaded MIL-88B(Fe) thin film, and d) Fe-MIL-88B thin film after drug releasing.

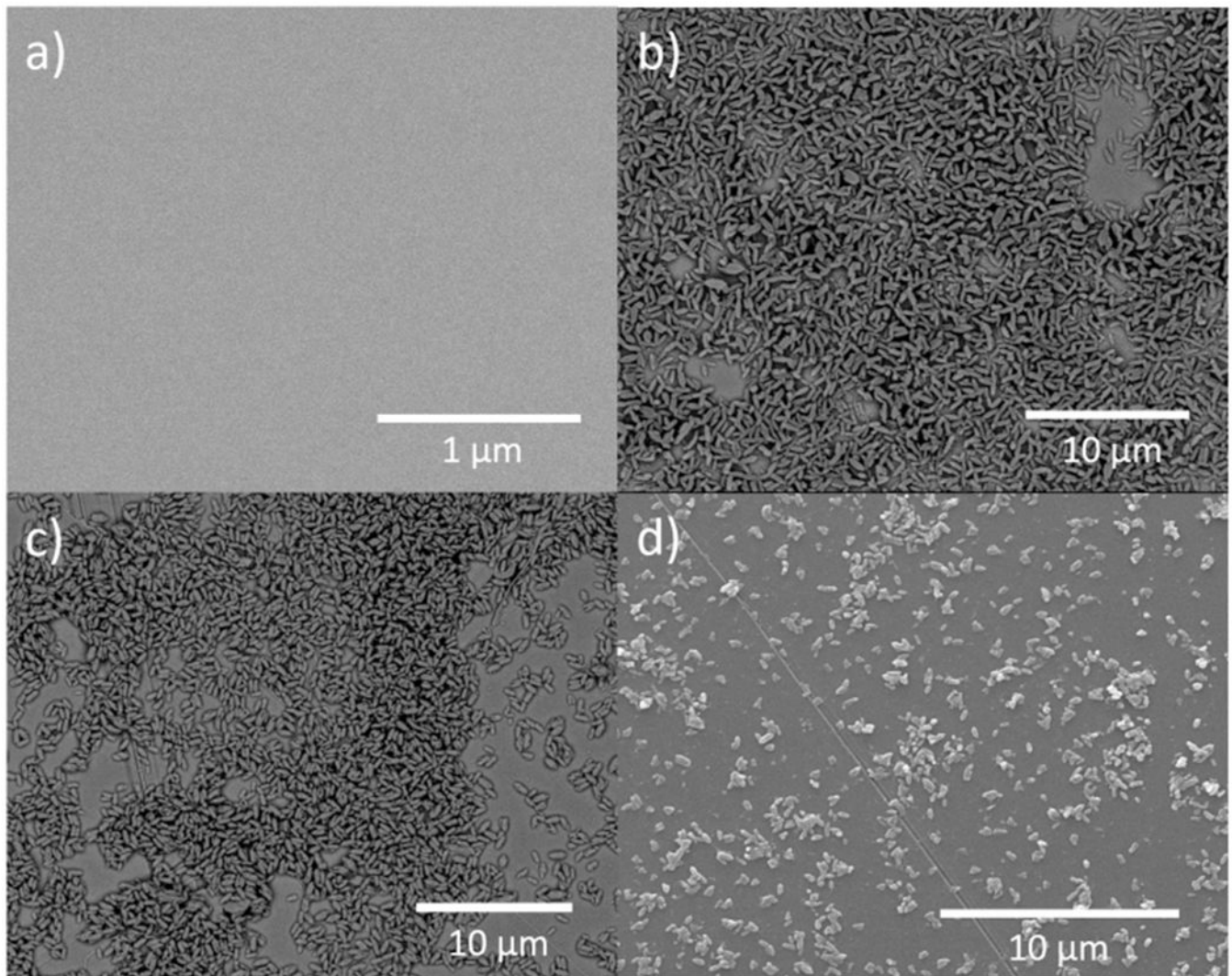


Fig. 3.

SEM images of a) MHDA-modified Au substrate, b) MIL-88B(Fe) thin film on a MHDA-modified Au surface, and ibuprofen loaded MIL-88B(Fe) before c) and after d) soaking in PBS for 6 h.

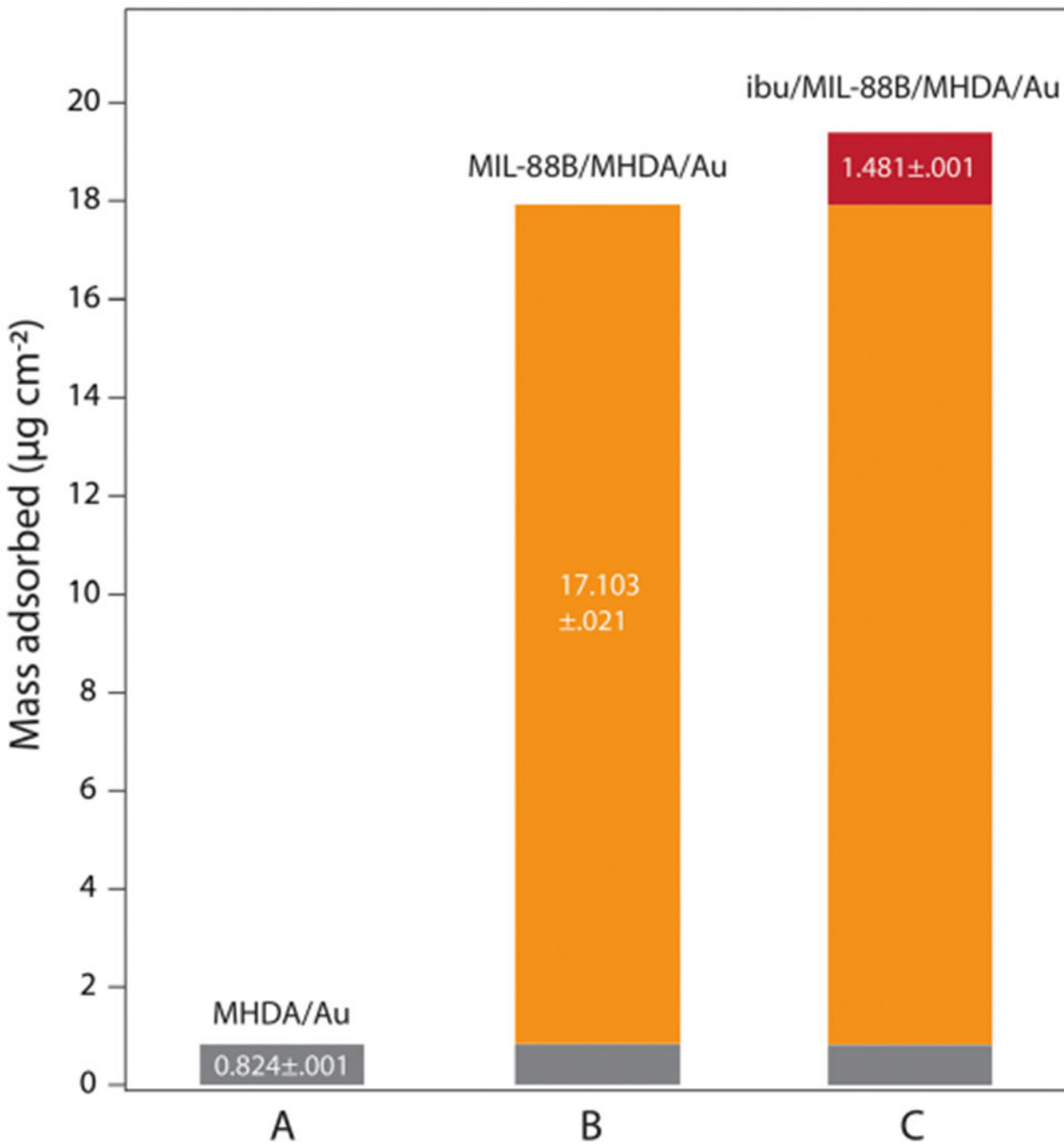


Fig. 4.

The mass change of a gold-coated QCM sensor calculated via Sauerbrey equation based on frequency changes after A) MHDA SAM modification, B) MIL-88B(Fe) fabrication, and c) ibuprofen loading in MIL-88B(Fe) thin film.

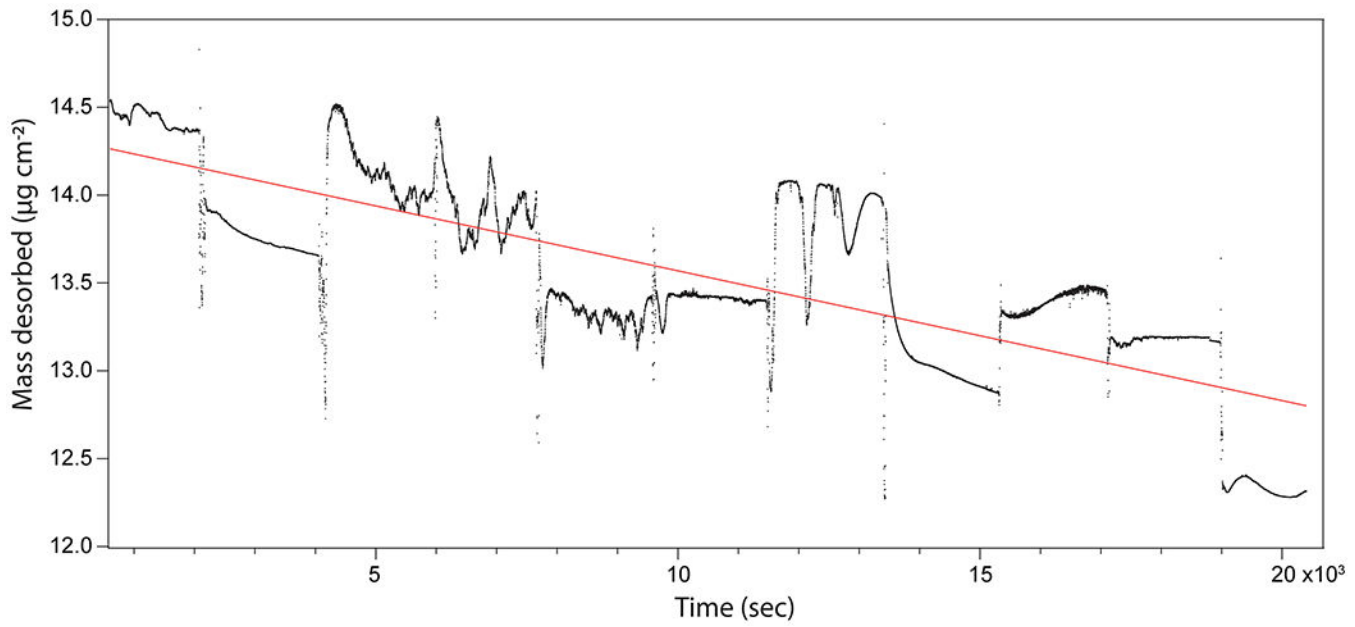
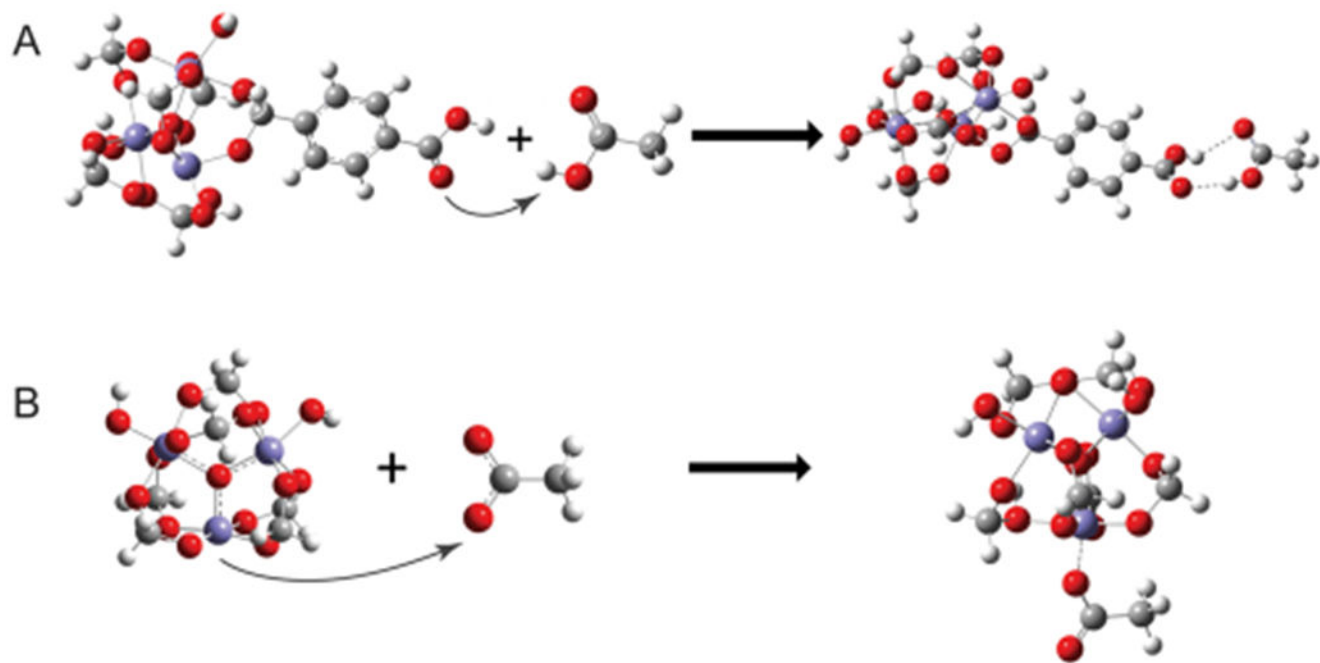


Fig. 5.

The mass changes of the ibuprofen loaded MIL-88B(Fe) on a modified Au QCM sensor as a function of time. Desorbed mass amount was calculated via Sauerbrey equation from the frequency measurements. The solid line indicates a linear trend fit to the experimental results shown in black dots.

**Fig. 6.**

Two competing models of bonding between MIL-88B(Fe) and the COOH-terminated SAM. In Model A, MIL-88B(Fe) cluster showcasing an explicit terephthalic acid linker forms hydrogen bonding to the carboxyl (COOH) end of MHDA. In Model B, the MIL-88(Fe) cluster has one open Fe site that is hypothesized to bind to the deprotonated carboxylate (COO-) end of MHDA in a coordination bond. Iron (purple), oxygen (red), carbon (gray), and hydrogen (white). (For interpretation of the references to colour in this figure legend, the reader is referred to the web version of this article.)

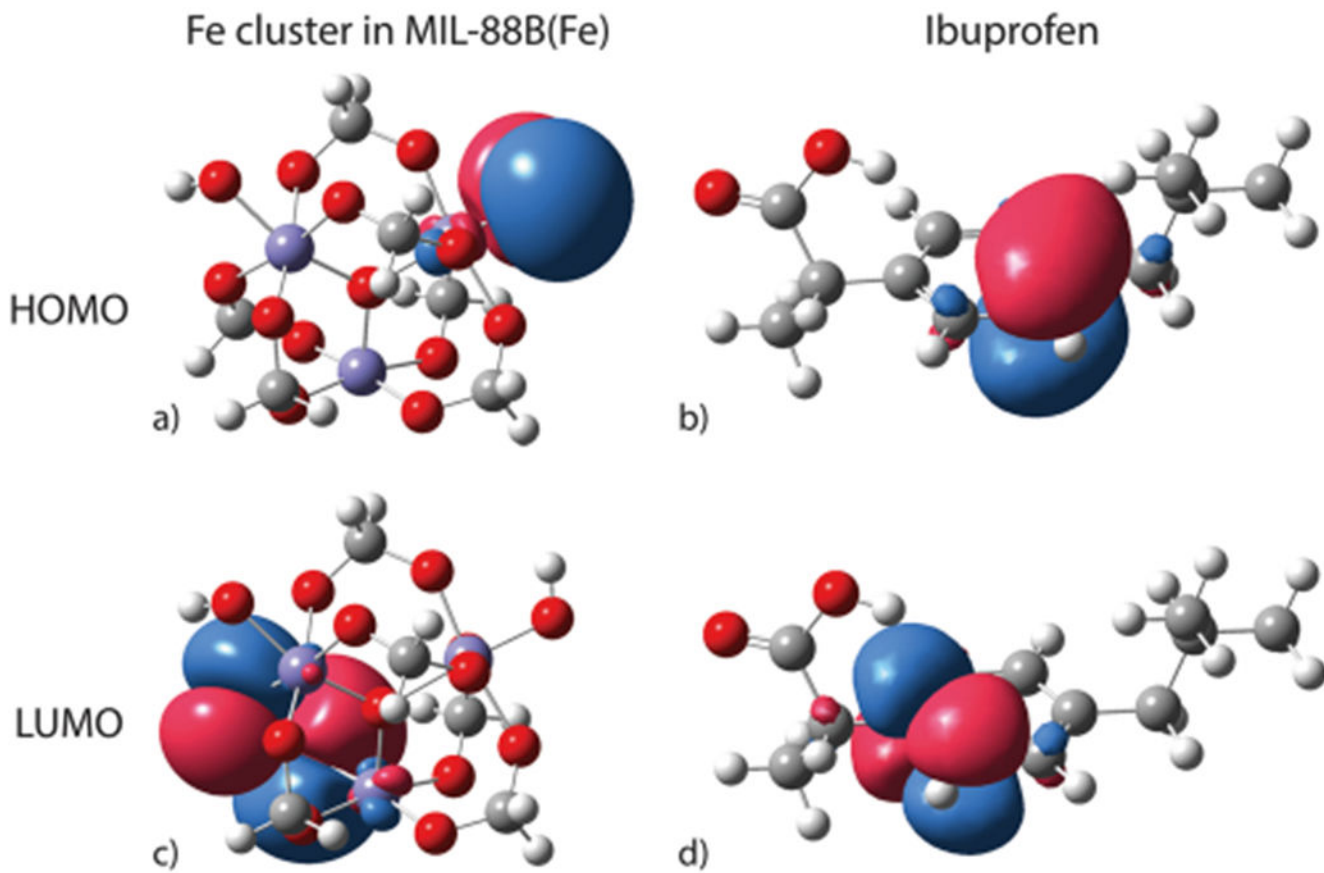
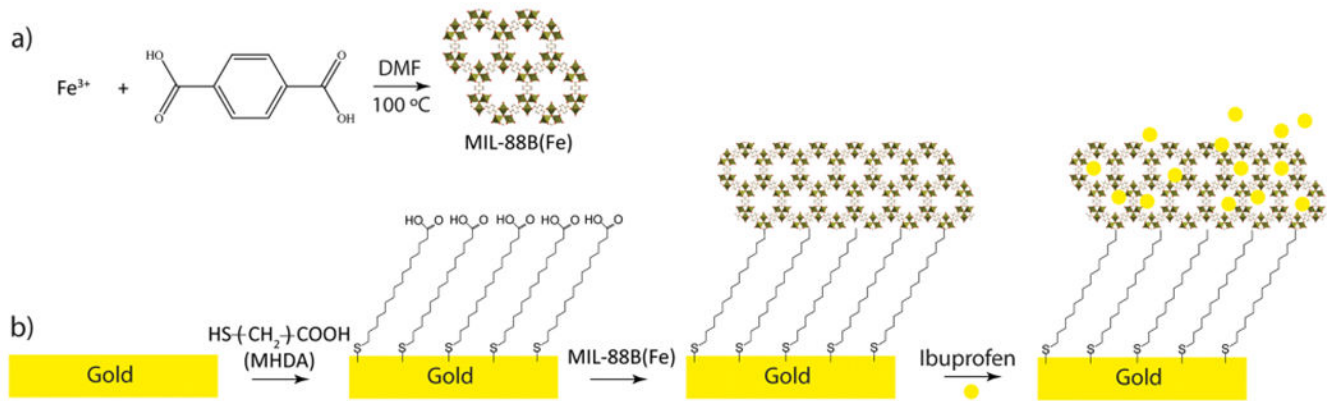


Fig. 7.

DFT computationally predicted HOMOs and LUMOs of the MIL-88B(Fe) cluster (a) & (c) and ibuprofen (b) & (d). MIL-88B(Fe) is represented by an unsaturated Fe trimer. Iron (purple), oxygen (red), carbon (gray), and hydrogen (white); positive and negative lobes are presented by red and blue color with an isosurface. (For interpretation of the references to colour in this figure legend, the reader is referred to the web version of this article.)

**Scheme 1.**

Schematic illustration of a) synthesis of bulk MIL-88B(Fe), and b) MIL-88B(Fe) film preparation on a COOH-terminated Au coated Si surface for drug loading with ibuprofen as a model drug. The silicon substrate is omitted for clarity. Ibuprofen was represented by solid yellow dots. (For interpretation of the references to colour in this figure legend, the reader is referred to the web version of this article.)